

1
2 **Contribution of water soluble**
3 **organic matter from multiple**
4 **marine geographic eco-regions**
5 **to aerosols around Antarctica**

6
7
8
9 Matteo Rinaldi¹, Marco Paglione¹, Stefano Decesari¹,

10
11 Roy M. Harrison^{2†}, David C.S. Beddows²,

12
13 Jurgita Ovadnevaite³, Darius Ceburnis³, Colin D. O'Dowd³,

14
15 Rafel Simó⁴, Manuel Dall'Osto^{4*}

16
17
18
19 ¹Institute of Atmospheric Sciences and Climate, National Research Council,
20 Bologna, Italy.

21
22 ²National Centre for Atmospheric Science, University of Birmingham,
23 Edgbaston, Birmingham, B15 2TT, United Kingdom

24
25 ³School of Physics and Centre for Climate and Air Pollution Studies, Ryan
26 Institute, National University of Ireland Galway, University Road, Galway,
27 Ireland

28
29 ⁴Institute of Marine Sciences, Passeig Marítim de la Barceloneta, 37-49. E-
30 08003, Barcelona, Spain;
31 corresponding author to Email: dallosto@icm.csic.es,
32

33
34 [†]Also at: Department of Environmental Sciences / Center of Excellence in
35 Environmental Studies, King Abdulaziz University, PO Box 80203, Jeddah,
36 21589, Saudi Arabia
37

38
39

40 **TOC**

41

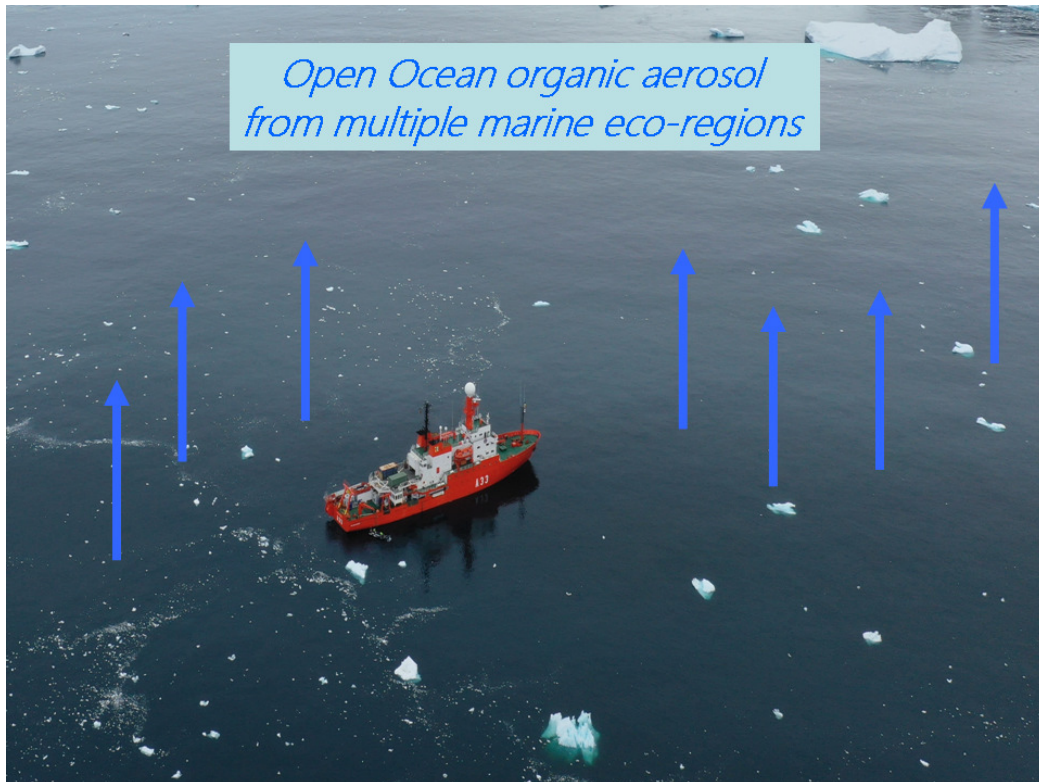
42

43

44

45

46



47

48

49

50

51

52

53

54

55

56

57

58

59 **Abstract**

60

61

62 We present shipborne measurements of size-resolved concentrations of
63 aerosol components across ocean waters next to the Antarctic Peninsula,
64 South Orkney Islands and South Georgia Island, evidencing aerosol features
65 associated to distinct eco-regions. Non-methanesulfonic acid Water Soluble
66 Organic Matter (WSOM) represented 6-8% and 11-22% of the aerosol PM₁
67 mass originated in open ocean (OO) and sea ice (SI) regions, respectively.
68 Other major components included sea salt (86-88% OO, 24-27% SI), non sea
69 salt sulfate (3-4% OO, 35-40% SI), and MSA (1-2% OO, 11-12% SI). The
70 chemical composition of WSOM encompasses secondary organic
71 components with diverse behaviors: while alkylamine concentrations were
72 higher in SI air masses, oxalic acid showed higher concentrations in the open
73 ocean air. Our online single-particle mass spectrometry data exclude a
74 widespread source from sea bird colonies, while the secondary production of
75 oxalic acid and sulfur-containing organic species via cloud processing is
76 suggested. We claim that the potential impact of the sympagic planktonic
77 ecosystem on aerosol composition has been overlooked in past studies, and
78 multiple eco-regions act as distinct aerosol sources around Antarctica.

79

80

81

82

83

84

85

86

87

88

89

90

91

92

93

94

95

1. Introduction

96

97

98 Remote from most human influences, the Southern Ocean (SO) is one of the
99 most pristine regions on Earth, and a window to the preindustrial atmospheric
100 conditions and processes¹⁻⁵. It is the stormiest of all oceans, and its
101 atmospheric and oceanic circulations impact the entire Southern hemisphere
102 and beyond. The surface of the ocean closer to the Antarctic continent
103 undergoes an annual freezing cycle, forming a layer of sea ice that generally
104 extends over an area ranging from 4×10^6 km² in the summer to approximately
105 19×10^6 km² in late winter¹. This large area increases surface albedo and
106 controls the air-sea gas exchange. Sea ice ecosystems are also one of the
107 largest biomes on earth, providing a stable habitat for diverse microbial
108 assemblages^{2,3}.

109 Currently, many unknowns remain about atmospheric and oceanographic
110 processes in this region, and their linkages. Climate models are prone to large
111 biases in the simulation of clouds, aerosols and air-sea exchanges⁴. This is
112 largely due to the poor understanding of aerosol sources and processes in
113 this region. Overall, two natural sources largely govern the aerosol population,
114 sea spray (primary) and non sea salt sulfate (nssSO_4^{2-} ; secondary). Sea
115 spray (mostly composed of sea salt) generated by breaking waves is often
116 reported as the main source of supermicron aerosols in marine areas^{6,7}.
117 Recently, blowing snow over pack ice has been suggested to contribute sea
118 salt aerosol in similar amounts to breaking waves⁸⁻¹⁰. The other major
119 component of Antarctic aerosols, nssSO_4^{2-} , is mainly derived from
120 atmospheric oxidation of dimethylsulfide (DMS), a trace gas produced by
121 marine plankton. The marine sulfur biogeochemical cycle received much
122 attention after the proposal by Charlson et al. (1987)¹² that the principal
123 source of cloud condensation nuclei (CCN) in the marine environment is
124 DMS-derived nssSO_4^{2-} ¹³. Such a hypothesis of a central role for DMS was
125 questioned by Quinn and Bates (2011)¹⁴ as the large variety of ocean-emitted

126 aerosol components was being disclosed, but mounting evidence has been
127 collected thereafter that DMS emission chiefly contributes to aerosol formation,
128 growth and activation as CCN over the oceans¹⁵⁻¹⁸. In the atmosphere, DMS
129 is oxidized also into aerosol-prone methanesulfonic acid (MSA), which peaks
130 in the summer and is found predominantly as methanesulfonate in the
131 submicron size range¹⁹. Unlike nssSO_4^{2-} , which may originate also from
132 anthropogenic and lithogenic sources, MSA has been proposed as a proxy for
133 oceanic DMS emissions. However, the overall interpretation of MSA and
134 nssSO_4^{2-} is far less straightforward than initially thought²⁰, given complex
135 ecological and biogeochemical processes controlling the DMS marine
136 emissions²¹ and variable MSA oxidation yields²².

137 The relative roles of secondary aerosols produced from biogenic sulfur versus
138 primary sea-spray aerosols in regulating cloudiness above the SO is still a
139 matter of debate²³⁻²⁷. Mc Coy et al. (2015)²⁵ reported observational data
140 indicating a significant spatial correlation between regions of elevated Chl-a
141 and particle number concentrations across the SO, and showed that modeled
142 organic mass fraction and sulfate explain $53 \pm 22\%$ of the spatial variability in
143 observed particle concentration, suggesting that primary marine organic
144 aerosols are important in this region, similarly to other remote marine
145 regions²⁸. Despite the increasing awareness of their importance,
146 measurements of organic components in SO aerosols are scarcer than
147 inorganic measurements, and the overall apportionment of primary versus
148 secondary marine aerosol in the southern hemisphere is not known. First
149 observations of organic carbon (OC) in size-segregated aerosol samples
150 collected at a coastal site in the Weddell Sea (Virkkula et al., 2006)²⁹ showed
151 that MSA represented only a few % of the substantial amount of OC observed
152 in the submicron fraction. However, Zorn et al (2008)³⁰ showed that MSA
153 dominated Antarctic OC, whereas non-MSA organic compounds dominated
154 SO OC. Recent measurements over the SO (43°S–70°S) and the Amundsen
155 Sea (70°S–75°S) showed that Water Insoluble Organic Carbon (WIOC)
156 accounted for 75% and 73% of aerosol total organic carbon in the two regions,
157 respectively³¹. In the Amundsen Sea, WIOC concentrations correlated with
158 the relative biomass of a phytoplankton species (*Phaeocystis antarctica*) that
159 produces extracellular polysaccharide mucus. Whilst sympagic and pelagic

160 plankton biomass controls biological productivity and the organic mass budget
161 of the Southern Hemisphere^{2,3}, including organic emissions to the atmosphere,
162 insular terrestrial biomass emissions contain large amounts of OC³²⁻³⁴.
163 Here, we report atmospheric measurements during a 42 day cruise in the SO
164 near Antarctica. We previously showed that the microbiota of sea ice and the
165 sea ice-influenced ocean can be a source of atmospheric organic nitrogen
166 (ON), specifically low molecular weight alkylamines³⁵. In a follow-up paper, we
167 reported a specific analysis of the primary ON aerosol detected by bubble
168 bursting chamber experiments on board, and also showed that alkylamines
169 form in the ambient aerosol by secondary processes involving volatilization
170 from the ocean surface and re-condensation onto acidic aerosol particles³⁶.
171 Using valuable high time resolution data from the same campaign, and
172 selecting 12 pseudo-steady state periods (where aerosol microphysical
173 properties varied less than 20% over eight hours), Fossum et al (2018)²⁷
174 evaluated the relative contributions of primary and secondary aerosols to SO
175 cloud condensation nuclei, and concluded that both sea salt and non-sea-salt
176 sulfate were major CCN components. In the selected cases studied, non MSA
177 organics contributed in the range 2-10% of aerosol mass.
178 In the present work, we (1) report the aerosol water soluble fraction
179 composition for the whole campaign; (2) report the size-resolved
180 concentrations of oxalic acid and alkyl amines in PM₁₀ aerosols; (3) discuss
181 the mixing state of oxalic acid by means of single particle mass spectrometry;
182 and (4) discuss the processes and sources responsible for the measured
183 patterns, stressing that multiple eco regions govern the aerosol population
184 numbers and composition. Such detailed chemical characterization of the
185 water soluble fraction of marine aerosol, including tracers of secondary
186 aerosol formation processes, has never been achieved before close to the
187 Weddell Sea region. We highlight that water soluble aerosol components
188 contribute to aerosol hygroscopicity and influence the ability of particles to
189 activate into cloud droplets, therefore being climate relevant. The role of
190 water-soluble organics in these processes in the Antarctic atmosphere is far to
191 being understood, mainly due to the lack of quantitative observations.
192

2 Methodology

195 **The Cruise.**

196 We conducted extensive aerosol measurements on board of the RV
197 Hesperides from January 2 to February 11, 2015 under the project PEGASO
198 (Plankton-derived Emissions of trace Gases and Aerosols in the Southern
199 Ocean). Different air masses were sampled, including the regions of Antarctic
200 Peninsula, South Orkney, and South Georgia Islands.

202 **Aerosol offline measurements.**

204 Off-line aerosol samples were collected on the upper deck by using a 5-stage
205 Berner impactor (hereafter BI5; type LPI80, Hauke; cut-offs at 0.06, 0.14, 0.42,
206 1.2, 3.5 and 10 μm) and a high volume PM_{10} sampler (hereafter HIVOL;
207 TECORA). Ion chromatography was used for the quantification of water-
208 soluble inorganic ions, oxalic acid and low molecular weight alkyl-amines
209 (methyl-, ethyl-, dimethyl-, diethyl- and trimethylamine)³⁷ in the BI5 water
210 extracts, while an elemental analyzer (Shimadzu TOC-5000A) was used to
211 quantify the water-soluble organic carbon content both of the impactor stages
212 and of the HIVOL filters. The water soluble organic carbon content was
213 measured on both kinds of samples to assess the impact of the sampling
214 technique upon the measured value. Indeed, impactor samples may be
215 subject to negative artifacts due to loss of semi-volatiles at the low operating
216 pressure and to bouncing, while HIVOL samples on quartz filters may be
217 affected by positive artifacts³⁸.

218 Sampling was allowed only when the samplers were upwind the ship exhaust
219 with a relative wind speed threshold of 5 m s^{-1} . Due to the necessity of
220 collecting sufficient amounts of samples for detailed chemical analyses,
221 sampling time was of the order of ~ 50 h for each sample. Samples were
222 stored at -20 °C until the chemical analyses. One field blank per sample was
223 collected during the cruise and the concentrations were corrected for the
224 blank values, which resulted negligible for amines and oxalate. A carbon-to-
225 mass conversion factor of 2 was used to estimate the WSOM from organic

226 carbon measurements. This value is in line with state-of-the-art marine
227 organic aerosol measurements³⁹. The non-sea-salt fraction of aerosol
228 chemical components was derived based on the standard seawater chemical
229 composition using Na⁺ as the sea-salt tracer.

230

231 **Aerosol online measurements.**

232

233 The online instruments³⁴ were kept inside the bow of the ship, sampling was
234 done with an purposely designed inlet, 9m in length followed by a cyclon with
235 a cut-off of approximately 5µm at a flow rate of 5 L min⁻¹. All downstream
236 online instruments were isokinetically subsampling from it and dried to below
237 40% relative humidity. The ATOFMS (model 3800-100, TSI, Inc.) allowed
238 collection of mass spectra (both positive and negative) of single particles
239 roughly between 500 and 1500 nm. The ATOFMS mass spectra were
240 imported into Yet Another ATOFMS Data Analyzer (YAADA), and adaptive
241 resonance theory neural network, ART-2a (learning rate 0.05, vigilance factor
242 0.85, and 20 iterations) was run⁴⁰. The size resolved non-refractory chemical
243 composition of submicron aerosol particles was measured with an Aerodyne
244 High Resolution Time of Flight Aerosol Mass Spectrometer (HR-ToF-AMS,
245 Aerodyne, Billerica, MA)⁴¹, hereafter indicated as AMS.

246

247

248 **Bioregion classification**

249

250 We collected aerosol data in the areas of the Antarctic Peninsula, South
251 Orkney, and South Georgia Islands. We ran 117 air mass back trajectories
252 (6h resolution, 42 days) and classified them into two broad source regions
253 according to the characteristics of the overflown areas: “open ocean” (OO)
254 and “sea ice” (SI). Out of the 6 samples analyzed, PE24, PE28 and PE06
255 were assigned to OO, and PE09, PE13 and PE18 were assigned to SI³⁵. A
256 detailed characterization of the air mass history, ground type contribution and
257 water soluble organic features of each sample have been presented in
258 Decesari et al.⁴², where a map of the sampling locations can also be found.
259 As we have previously showed^{35,36,42}, SI samples are influenced by aerosol

260 precursors emitted by the peculiar microbiota thriving in sea ice and sea ice-
261 influenced waters, while OO samples are representative of the open Ocean
262 biota. This results in distinct chemical compositions, which we will investigate
263 in detail below.

264

265 **3 Results**

266

267 **3.1 Overall aerosol chemical composition**

268

269 Six shipborne aerosol filters are reported in this study. Figure SI1 and SI2
270 show the remarkable similarity among the sub-micron OO and SI samples
271 (within the same group).

272 The average concentrations of the PM₁ aerosol water soluble fraction in the
273 OO and SI samples are shown in Figure 1 and reported in Tables SI1. Sea
274 salt dominates the PM₁ water soluble fraction in OO samples, with average
275 concentrations of $2.39 \pm 2.36 \mu\text{g m}^{-3}$ (n=3; min, max: 0.79-5.1 $\mu\text{g m}^{-3}$)
276 representing on average 87% of the mass. In the SI region, sea salt
277 concentrations were ten fold lower, average of $0.198 \pm 0.056 \mu\text{g m}^{-3}$ (n=3; min,
278 max: 0.143-0.254 $\mu\text{g m}^{-3}$), representing on average only 25% of the aerosol
279 water soluble mass. By contrast, in the SI region the dominant species was
280 nssSO_4^{2-} , with average concentrations of $0.295 \pm 0.061 \mu\text{g m}^{-3}$ (n=3; min, max:
281 0.228 - $0.348 \mu\text{g m}^{-3}$) representing on average 37% of the water soluble
282 fraction. This was the third lowest species in OO air masses, with average
283 concentrations of $0.099 \pm 0.014 \mu\text{g m}^{-3}$ (n=3; min, max: 0.087-0.114 $\mu\text{g m}^{-3}$)
284 representing on average only 4% of the aerosol water soluble mass.

285 As expected, MSA exhibited similar patterns to nssSO_4^{2-} . Higher
286 concentrations were seen from the SI region, with average concentrations of
287 $0.088 \pm 0.032 \mu\text{g m}^{-3}$ (n=3; min, max: 0.061-0.123 $\mu\text{g m}^{-3}$) representing on
288 average 11% of the water soluble fraction. High MSA concentrations over the
289 Weddell Sea were previously attributed to emissions from the margine ice
290 zone biota^{35,36,42} in agreement with the global MSA climatology⁴³. In the OO
291 region, average concentration was $0.043 \pm 0.012 \mu\text{g m}^{-3}$ (n=3; min, max: 0.036-
292 $0.057 \mu\text{g m}^{-3}$), representing on average 2% of the aerosol water soluble mass.

293 Minor concentrations of ammonium were found for the SI region, average of
294 $0.068 \pm 0.017 \mu\text{g m}^{-3}$ ($n=3$; min, max: 0.055 - $0.087 \mu\text{g m}^{-3}$), which represented
295 on average 9% of the water soluble fraction ($n=3$; min, max: 7-10%). These
296 were much lower in the OO region, as previously discussed in Dall'Ósto et al.
297 (2017)³⁵: average of $0.027 \pm 0.005 \mu\text{g m}^{-3}$ ($n=3$; min, max: 0.022 - $0.031 \mu\text{g m}^{-3}$),
298 representing on average 2% of the water soluble mass ($n=3$; min, max: 0-3%).
299 Low ammonium concentrations made the submicron aerosol particles rather
300 acidic as in many other remote regions.

301 A key observation was that non-MSA organic compounds (see Methods)
302 represented an important aerosol component. The average non-MSA WSOM
303 concentration from the BI5 was $0.083 \pm 0.022 \mu\text{g m}^{-3}$ ($n=3$; min, max: 0.058 -
304 $0.10 \mu\text{g m}^{-3}$) and 0.17 ± 0.02 ($n=3$; min, max: 0.15 - $0.19 \mu\text{g m}^{-3}$) in SI and OO
305 regions, respectively, while from the HIVOL samplers concentrations as high
306 as 0.19 ± 0.05 (SI, $n=3$; min, max: 0.21 - $0.22 \mu\text{g m}^{-3}$) and 0.21 ± 0.05 (OO, $n=3$;
307 min, max: 0.17 - $0.26 \mu\text{g m}^{-3}$) were obtained. Consequently, non-MSA-WSOM
308 accounted for 11% ($n = 3$; min, max: 9-16%) and 6% ($n=3$; min, max: 3-13%)
309 of total sub-micrometer water soluble mass in SI and OO regions, respectively,
310 when considering the BI5 results, and 22% ($n=3$; min, max; 18-27%) and 8%
311 ($n=3$; min, max: 4-15%), using the HIVOL data. Although the concentration
312 differences between the two datasets are notable (particularly for the Si
313 region), the non-MSA WSOM was the third most abundant component in SI,
314 and the second in OO, independent of the sampling technique.

315 Parallel AMS measurements performed during the cruise^{27,35} were averaged
316 over the filter sampling times in order to provide a further evaluation of the
317 organic aerosol concentration over the two regions. An excellent agreement
318 was observed for MSA concentrations between AMS and BI5 samples ($n = 6$;
319 slope: 1.04; R: 0.66), while more significant differences were reported for the
320 total organics. Comparing the non-MSA organic aerosol concentration by
321 AMS with the non-MSA-WSOM measured on the BI5 samples, we got a slope
322 of 0.53 ($n=6$; R: 0.74, OM/OC = 2, see Par. 2.), indicating at least a factor two
323 overestimation of the organic fraction on the BI5 samples with respect to AMS
324 measurements. The overestimation was obviously higher if we compare the
325 AMS with the HIVOL samples ($n=6$; slope: 0.33, R: 0.56). Accordingly, if we
326 assume that all the organics measured by the AMS contribute to the WSOM

327 measured offline, a reduction of the average non-MSA WSOM contribution
328 over the SI region is obtained, from the range 11-22% by offline
329 measurements, down to 8%.

330 This discrepancy between the sub-micrometre non-MSA organic aerosol
331 quantification by offline and online techniques is consistent with the existing
332 literature. Virkkula et al. (2006)²⁹ reported a high contribution of non-MSA
333 organics in Antarctic samples (~50% of PM₁ mass) by offline chemical
334 analyses, while Zorn et al. (2008)³⁰ reported a negligible non-MSA organic
335 contribution in sub-micrometre Antarctic aerosol through online AMS
336 measurements. Although the existing measurements are too scarce to derive
337 any sound conclusion, the evidenced tendency is worthy of investigation and
338 proves the necessity for further organic aerosol characterization studies over
339 Antarctica.

340 Considering the PM₁₀ size range (Table SI2), sea salt dominated in both OO
341 and SI samples, with average concentrations of 7.93±3.99 µg m⁻³ (n=3; min,
342 max: 5.20-12.51 µg m⁻³) and 2.17±0.83 µg m⁻³ (n=3; min, max: 1.22-2.77 µg
343 m⁻³) respectively, representing on average 94 and 78% of the aerosol water
344 soluble mass.

345 Whilst the speciation of individual organic compounds was treated in a
346 separate paper⁴², the next section discusses two chemicals of interest as
347 markers of secondary aerosol sources.

348

349 **3.2 Alkylamine and oxalate measurements**

350

351 In this Section, we present the atmospheric concentrations of selected
352 secondary aerosol formation process tracers: alkyl amines and oxalic acid.
353 The former have been associated to secondary aerosol formation based on
354 acid-base reactions³⁷, including new particle formation³⁵. The latter was
355 identified as one of the most abundant single oxygenated compounds in many
356 marine aerosol studies at different latitudes⁴⁴⁻⁴⁸. All the tracers were
357 characterized by high quantification precision even at the low aerosol
358 concentrations typical of Antarctica.

359

360 **3.2.1. Aerosol size-resolved mass concentrations**

361

362 Figure 2 shows that alkylamines were 5 times higher (t-test, significantly
363 different, $p < 0.01$) in aerosols from the SI region ($n=3$; $9.1 \pm 4.5 \text{ ng m}^{-3}$) than
364 from the OO regions ($n=3$; $1.8 \pm 1.1 \text{ ng m}^{-3}$). In a previous paper³⁵ we had
365 reported alkylamines only in PM_1 aerosols, here we present the PM_{10}
366 concentrations. Contrasting with the amines, oxalate concentrations were 9
367 times higher (t-test, significantly different, $p < 0.05$) in OO ($n=3$; $1.98 \pm 1.44 \text{ ng}$
368 m^{-3}) than in the SI ($n=3$; $0.20 \pm 0.09 \text{ ng m}^{-3}$) region (Figure 2a).

369 Concerning their size distributions, clear differences were seen (Figure 2b).
370 Whilst amines occurred mainly in the fine mode, the oxalate size distribution
371 was different between regions. In SI samples, the sub-micron oxalate
372 concentration was below detection limit in two samples out of three, while
373 non-negligible concentrations were always detected in the $1.2\text{--}3.5 \mu\text{m}$ size
374 range, resulting in the coarse-mode dominated distribution of Figure 2. In OO
375 samples, the oxalate distribution peaked in fine particles ($0.42\text{--}1.2 \mu\text{m}$). Very
376 few measurements of oxalate in the SO exist. Xu et al (2013)⁴⁹ reported low
377 concentrations, $3.8 \pm 3.8 \text{ ngm}^{-3}$ (range: 0 to 9.1), over the SO, and 2.2 ± 1.5
378 ngm^{-3} (range: 0 to 4.6) over coastal Antarctica. These results were in line with
379 data collected in Aboa Station²⁹ and in the region of $>50^\circ\text{S}, 130^\circ\text{E}\text{--}150^\circ\text{E}$ ⁴⁹. In
380 this latter study, oxalate size distributions over the SO were bimodal, with
381 peak at $<0.49 \mu\text{m}$ and $0.95\text{--}1.5 \mu\text{m}$, whereas over coastal East Antarctica
382 oxalate concentration peaked at $0.56\text{--}1.8 \mu\text{m}$.

383

384 **3.2.2 Mixing state of oxalate containing particles**

385

386 In this section we investigate the aerosol mixing state, broadly defined as the
387 distribution of the chemical component within the aerosol population. In
388 Dall'Osto et al., (2019)³⁶ we compared ATOFMS spectra of particles
389 generated by bubbling melted sea ice with those produced by bubbling
390 surface sea water. Here, we only consider the mass spectra of ambient
391 aerosols. We expanded the analysis by running ART-2a on mass spectra
392 containing a peak (m/z -89, $[(\text{C}_2\text{O}_4\text{H})\text{H}]^-$, approximately 1,300 single particle
393 mass spectra) representative of oxalic acid⁵¹. The small peak at m/z 179 is
394 attributed to the oxalic acid dimer $[(\text{C}_2\text{O}_4\text{H})_2\text{H}]^-$, which is commonly observed

395 in the spectra of oxalic acid standards. Unfortunately, the temporal trends of
396 the ATOFMS particles detected did not allow differentiation of the SI and OO
397 regions due to low counts and poor statistic. Nevertheless - broadly - three
398 particle types were seen:

399 (a) ATOOFMS Na-OX (about a quarter of the total mass spectra identified): Sea
400 spray particles containing organic carbon including oxalic acid. Peaks at m/z
401 23 (Na^+), m/z 24 (Mg^{++}), m/z 39 (K^+) (positive mass spectra) and m/z -16 [O^-],
402 -17 [OH^-], -35 (Cl), -46 [Na_2^-], 62 [Na_2O^+], and 63 [Na_2OH^+] consistent with
403 sea salt in sea spray (Figure 3a). The negative ion mass spectrum shows
404 prominent peaks at m/z -26 [CN^-] and m/z -42 [CNO^-], indicating that all
405 particle types presented were internally mixed with organo-nitrogen species.
406 In the negative spectra, putative peaks of oxalate (m/z -89) are seen also with
407 larger mass peaks, likely due to unidentified large chemical compounds. This
408 particle type likely corresponds to degraded primary marine organic aerosols
409 internally mixed with sea spray.

410 (b) ATOOFMS biogenic-OX (about a quarter of the total mass spectra identified).
411 Peaks due to Na^+ (m/z 23), K^+ (m/z 39) and phosphate (m/z -63 [PO_2^-] and
412 m/z -79 [PO_3^-]) characterize this particle type (Figure 3b). The ATOFMS has
413 already proved to be a good tool to separate dust (mainly Ca-rich or Al-Si rich)
414 and biological particles^{52,53}. Briefly, biological mass spectral signatures can be
415 differentiated from crustal dust on the basis of abundant organic and
416 phosphorus ions, as well as a lack of key dust markers, such as aluminium
417 and silicates. Additionally to the peak of oxalate (m/z -89) a strong peak at m/z
418 114 can be seen, previously demonstrated to be preserved in particles that
419 contain amine salts and that have undergone photo-oxidation^{54,55}. This
420 particle type may correspond to biogenic material in general, but not enough
421 mass spectra (about a dozen) were collected to obtain more information.

422 (c) ATOOFMS SOA-OX (about half of the total mass spectra identified). This
423 particle type was seen associated with secondary organic components in both
424 positive and negative mass spectra (Figure 3c). Beside the previously
425 described peaks associated with amines and oxalic acid, a unique peak at m/z
426 59, ($[\text{N}(\text{CH}_3)_3]^+$) is attributed to trimethylamine (TMA). Previous studies
427 showed that cloud/fog processing can increase gas-to-particle partitioning of
428 TMA⁵⁶, and potentially form non-salt organic aerosols⁵⁷. The unique mass

429 series of m/z -81, -97 and m/z -111 is due to species $[\text{HSO}_3]^-$, $[\text{HSO}_4]^-$ and
430 $[\text{HOCH}_2\text{SO}_3]^-$. ATOFMS particle spectra of this type have previously been
431 shown to arise from hydroxymethanesulphonate in both laboratory studies
432 and field experiments^{58,59}. Minor peaks can also be seen at m/z 58, 74, and
433 128, which were previously attributed to alkyl ammonium nitrate salt particles
434 formed by reaction of nitric acid and amines⁶⁰.
435 Our ATOFMS mixing state results confirm that a complex mixture of oxalate
436 containing particles contributes to the chemical composition of Antarctic
437 aerosol, including primary Na-containing aerosols and non-MSA marine
438 secondary organic particles.

439

440

441 **4 Discussion**

442

443 WSOM was found present in non-negligible concentration during our study,
444 although with significant uncertainty due to its dependence on the
445 measurement technique. Even though alkylamines and oxalic acid altogether
446 represented a minor fraction of the total water soluble organic mass (see
447 Tables SI1 and SI2), these compounds can be used as proxies to discuss
448 processes and sources of secondary organic aerosols in the study area.

449

450 **4.1 Multiple processes driving the observed aerosols patterns**

451

452 **4.1.1 Amines**

453

454 Aliphatic amines are known important organic compounds in the marine
455 atmosphere. An important contribution of biogenic amines to marine organic
456 aerosol was first reported by Facchini et al. (2008)³⁷, pointing to a secondary
457 formation pathway for alkylammonium salts. Indeed, in our study the size
458 distribution peaked in the accumulation mode and exhibited a good correlation
459 with nssSO_4^{2-} , NH_4^+ and MSA, which is indicative of an acid-base reaction of
460 gaseous amines with sulfuric or sulfonate acids. In our previous study³⁵ we
461 demonstrated that the microbiota of sea ice and the sea ice-influenced ocean

462 is a source of atmospheric organic nitrogen, including low molecular weight
463 alkylamines. In a follow up study³⁶, thermodynamic equilibrium calculations
464 suggested that the alkylamine shift from seawater to atmospheric secondary
465 aerosol is driven by the very low pH expected in fine and ultrafine particles.
466 Furthermore, a detailed analysis of single particle mass spectra of sea-spray
467 (primary) aerosols artificially generated by bubbling seawater samples
468 showed that in ambient aerosol the fingerprint of primary alkylamine-rich
469 particles represents only a minor percentage (11-25%). Here we report an in-
470 depth analysis of total aerosol mass as well as the size distribution of
471 alkylamines, which show that these compounds occur in different aerosol
472 modes from oxalic acid.

473 It should be kept in mind that ammonia and organic nitrogen in general -
474 including alkylamines - may also be important contributors to new particle
475 formation and growth in the SO. Indeed, using an unprecedented suite of
476 instruments, Jokinen et al. (2018)⁶¹ showed that ion-induced nucleation of
477 sulfuric acid and ammonia, followed by sulfuric acid-driven growth, is the
478 predominant mechanism for new particle formation and growth in eastern
479 Antarctica a few hundred kilometers from the coast⁶¹. Dall'Osto et al (2017)³⁵
480 suggested that the microbiota of sea ice and sea ice-influenced ocean were a
481 significant source of atmospheric nucleating particles (size of 1-3nm). It must
482 be noted, though, that new particle formation and growth is a key process that
483 governs particle number concentrations but does not play an important role in
484 governing aerosol mass.

485

486 **4.1.2 Oxalate**

487

488 Our study supports the existence of a natural source of oxalic acid to the
489 marine atmosphere^{62,63}. Previous studies^{44,62,63, 64, 65} showed that oxalate was
490 distributed along a wide aerosol size range, including the sub-micrometer and
491 a super-micrometer mode. This suggests that oxalate of marine origin must be
492 produced through a combination of processes. These may include:

493 (1) Cloud processing - from oxidation of gaseous glyoxal and mediated by
494 particulate water, occurring over remote oceanic regions, which may
495 contribute oxalate to submicrometer aerosols^{44,45, 46, 66, 67}.

496

497 (2) Photochemical degradation of fatty acids of biological origin at the ocean's
498 surface, giving rise to oxalic acid and other LMW dicarboxylic acids; these
499 may be transferred with sea-spray particles to the atmosphere and
500 subsequently degraded^{46, 48, 65, 68}.

501

502 (3) Neutralization of gaseous oxalic acid (which may originate from points (1)
503 or (2)) onto sea-salt particles⁴⁴.

504

505 The broad size distributions of oxalate in the OO region strongly points to
506 multiple atmospheric processes, in agreement with previous open sea
507 observations⁶. By contrast, the oxalate size distribution found in the SI region -
508 centered in the coarse mode at 1.2-3.5 μm - could be due to the degradation
509 of primary biogenic organic matter, emitted with sea spray^{62,63}. According to
510 this hypothesis, the limited importance of sea-spray emissions over the
511 Weddell Sea^{35,36} may explain the lower oxalate concentrations observed in SI
512 samples with respect to OO ones. On the other hand, in Dall'Osto et al.
513 (2019)³⁶ we have shown that sub-micron aerosol over the Weddell Sea is
514 extremely acidic, because of the persistent fine-mode sulfate and
515 methanesulfonic acid particles and the low liquid water content (LWC) (pH_{SI}
516 = 1.4; pH_{OO} = 6.6). The coarse size distribution of oxalate in this region may,
517 therefore, be driven by the fine aerosol acidity, which would favour the
518 accumulation of oxalate in the more alkaline coarse mode⁶⁹. This is the
519 simplest explanation, which probably accounts for much of the best known
520 mechanism pattern in the oxalic acid size distribution.

521 It is also possible that alternative pathways exist, including cloud and fog
522 processing, as discussed in point (1) above. An example of a real time event
523 of this process was recorded in the evening of the 14th January 2014 and it is
524 presented in Figure S14. The two aerosol size distribution modes indicative of
525 cloud processing⁷⁰ can be observed during the event. This event occurred in

526 the marginal sea ice region, the research vessel was about 75Km from the
527 closest coast of the little island of Coronation (South Orkneys). Figure SI5
528 shows that all air masses were travelling over open ocean and not terrestrial
529 zones before arriving at the ship. Furthermore, the case study was seen in air
530 masses that were the most affected by sea ice and the marginal sea ice zone
531 (Fig. SI5). A clear growth of the smaller mode from 38nm to 43nm was seen
532 over five hours (1 nm h^{-1} ; not shown), in concomitance with an increase of
533 Relative Humidity due to foggy-cloudy conditions. By contrast, the decrease of
534 the larger mode (from 105 nm to 87 nm) was likely due to the higher activation
535 of large aerosol due to higher RH. Immediately after the onset of fog, the
536 number of ATOFMS counts attributed to the SOA-OX particle type increased.
537 After the event, the two size modes returned to about 38-40 nm and 181-190
538 nm. The latter mode was likely due to cloud processing (Hoppel mode⁷⁰),
539 which transforms organic and inorganic compounds and shifts the size
540 distribution to large accumulation mode sizes. After about 4-7am on the 15th
541 January 2015 air masses changed, shifting towards West Pacific air masses,
542 hence different aerosols were sampled and the event track was lost.
543 Recently, Kim et al., (2019)⁷¹ demonstrated that aqueous reactions in
544 atmospheric droplets can significantly modify aerosol composition and
545 contribute to the formation of oxygenated and nitrogen-containing organic
546 compounds in atmospheric aerosol particles. Our study shows that chemical
547 reactions involving organic compounds of biogenic origin (acid-base
548 neutralization and oxidation reactions) - likely related to marginal sea ice
549 zones - are also occurring in the Antarctic region, and aerosol chemical
550 composition may be more complex than solely sulfate and sea spray.

551

552 **4.2 Marine vs terrestrial inputs of ammonia, amines and organic aerosol**

553

554 According to our previous studies^{35,36}, elevated alkylamine concentrations
555 originate from melted sea ice and sea-ice-influenced waters. These could
556 result from degradation of quaternary amine osmolytes, which we also found
557 in sympagic plankton. Regarding oxalate, the higher abundance in OO
558 samples suggests that this aerosol component is less related to the coastal
559 and marginal sea-ice zone.

560 An important open question for Antarctic aerosol is the relative role of marine
561 versus terrestrial sources of organic matter (including organic nitrogen) and
562 ammonia, whose answer is obscured by the scarcity of existing
563 measurements. Recently, Liu et al (2018)³⁴ showed that atmospheric aerosol
564 natural organic matter (OM) from a coastal location was 150 times higher in
565 summer than in winter. Natural sources that included marine sea spray and
566 seabird emissions contributed 56% OM in summer but only 3% in winter. The
567 “marine source” was identified by high hydroxyl group fractions, and the
568 “seabird source” was related to ammonium and an organic nitrogen peak
569 associated with coastal penguin emissions³⁴. In Bird Island, South Georgia,
570 Schmale et al. (2013)³³ also showed strong influence of sea bird colonies.
571 Legrand et al. (2012)⁷² reported oxalate enrichment in aerosols at Dumont
572 d’Urville Station, which was associated with the high levels of gaseous
573 ammonia in the atmosphere. It was suggested that seabirds and mammals in
574 coastal Antarctica could be sources of aerosol oxalate. This idea had also
575 been discussed in Legrand et al. (1998)⁶¹, where ornithogenic soil was
576 proposed to be a source of oxalate in aerosols. Therefore, oxalate would be
577 produced and released together with ammonia upon bacterial decomposition
578 of uric acid. However, it was also stressed that the relationship between
579 gaseous nitrogen (or carbon)-derived species and emitted oxalate aerosol
580 was likely a complex one⁷³⁻⁷⁴. Legrand et al. (1998)³² and Jourdain and
581 Legrand (2002)⁶⁷⁵ proposed $nssK^+$ and $nssCa^{2+}$ as tracers for ornithogenic
582 soil (defined as guano-enriched soil) emissions. Based on the proposed
583 metrics, we can exclude any significant contribution from bird colony
584 emissions in SI and, more obviously OO, samples. In fact, the K^+/Cl^- weight
585 ratio in SI and OO samples is 0.021 ± 0.003 and 0.020 ± 0.002 , respectively,
586 much closer to the seawater value (0.021) than to the proposed values for
587 ornithogenic soils (0.23-1.4). Similarly, the Ca^{2+}/C^- weight ratio is 0.026 ± 0.002
588 and 0.026 ± 0.0003 , against a seawater reference value of 0.021 and an
589 ornithogenic soil value of 0.045. Finally, the formula for calculating the amount
590 of potassium related to ornithogenic soil emissions (K_{or}), proposed by
591 Jourdain and Legrand (2002)⁷⁵, yielded negative values in both SI and OO
592 samples, demonstrating a tendency for K^+ depletion and certainly not an
593 enrichment.

594 The results presented in this study, together with our previous works from the
595 same sampling cruise^{35,36,42} show that alkylamines and oxalic acid have
596 different spatially located sources in the investigated area, with the former
597 being more related to sympagic emissions connected with sea-ice melting and
598 sea-ice influenced waters, and the latter being more related to pelagic
599 emissions. This suggests that aerosol chemical composition, and likely
600 physical properties, is strictly related to the biological environment
601 characterizing the source region^{35,36,42}. Aerosol samples reported in this study
602 showed no major relation with seabird emissions, even though this does not
603 exclude that this source may be significant in other Antarctic coastal
604 environments (eco-regions).

605

606 **4.3 Considerations under a changing climate perspective**

607

608 The Antarctic region possesses a substantial spatial heterogeneity across
609 marine, terrestrial and freshwater biomes, with productivity and biodiversity
610 patchiness superimposed on strong environmental gradients⁷⁶. Warming
611 climate is posing one of the greatest threats to the Antarctic environment. The
612 Antarctic Peninsula has experienced one of the most rapid temperature rises
613 in the Southern Hemisphere⁷⁷. Antarctic terrestrial productivity and
614 biodiversity occurs almost exclusively in ice-free areas that cover less than
615 1% of the continent, although these could increase under a strongest forcing
616 scenario^{77,78}. Changes in the Antarctic environment will feed back to climate
617 by biosphere and cryosphere exchanges with the atmosphere. Antarctica
618 harbors extreme physical gradients such as those of incident solar radiation,
619 UV intensity, ice cover, ocean circulation and temperature, which change over
620 time as a consequence of global warming. The impacts of these changes on
621 marine and terrestrial life through nutrient availability, ecophysiological
622 adaptations, duration of the productivity and breeding seasons, migrations
623 and location of refugia will affect biogenic emissions to the atmosphere,
624 aerosol formation and aerosol-cloud interactions. Also physicochemical
625 transformations of organic matter, as through exposure of snow and the sea
626 surface microlayer to solar radiation⁷⁹ will impact the emission of climate-
627 active substances to the atmosphere. Future interdisciplinary studies using

628 emerging chemical and statistical analytical techniques are required to tease
629 out processes across spatial gradients of key environmental factors.

630

631 **Acknowledgements**

632

633 The study was supported by the Spanish Ministry of Economy through project
634 BIO-NUC (CGL2013–49020-R), PI-ICE (CTM2017–89117-R) and the Ramon
635 y Cajal fellowship (RYC-2012-11922), and by the EU through the FP7-
636 PEOPLE-2013-IOF programme (Project number 624680, MANU – Marine
637 Aerosol NUcleations), all to MD, and PEGASO (CTM2012-37615) to RS. We
638 wish to thank the Spanish Armada, and particularly the captains and crew of
639 the BIO A-33 Hesperides, for their invaluable collaboration. We are also
640 indebted to the UTM, and especially Miki Ojeda, for logistic and technical
641 support. The Spanish Antarctic Programme and Polar Committee provided
642 context and advice. The National Centre for Atmospheric Science NCAS
643 Birmingham group is funded by the UK Natural Environment Research
644 Council. The whole PEGASO team is also acknowledged.

645

646 **References**

647

648

649 (1) Cavalieri, D.J., Parkinson, C.L., Gloersen, P., Comiso, J.C. & Zwally,
650 H.J.. Deriving long-term time series of sea ice cover from satellite passive-
651 microwave multisensor data sets. *Journal of Geophysical Research*, **1999** 104,
652 15 803–15 814.

653

654 (2) Arrigo KR, Lizotte MP, Mock T. Primary producers and sea ice. *Science*,
655 **2010**, pp. 283–326

656

657 (3) Arrigo KR, van Dijken GL, Strong AL.. Environmental controls of marine
658 productivity hot spots around Antarctica. *J Geophys Res - Oceans* **2015**, 120:
659 5545–5565. doi: 10.1002/2015JC010888.

660

661 (4) Hamilton DS. Natural aerosols and climate: understanding the
662 unpolluted atmosphere to better understand the impacts of pollution. *Weather*.
663 **2015**;70(9):264–8.

664

665 (5) Carslaw, K. S., Lee, L. A., Reddington, C. L., Pringle, K. J., Rap, A.,
666 Forster, P. M., Mann, G.W., Spracklen, D. V., Woodhouse, M. T., Regayre, L.
667 A., and Pierce, J. R.: Large contribution of natural aerosols to uncertainty in
668 indirect forcing, *Nature*, **2013**, 503, 67–71,
669 <https://doi.org/10.1038/nature12674>

670

671 (6) Rinaldi, M., Decesari, S., Finessi, E., Giulianelli, L., Carbone, C., Fuzzi,
672 S., O'Dowd, C. D., Ceburnis, D. and Facchini, M. C.: Primary and secondary
673 organic marine aerosol and oceanic biological activity: Recent results and 5
674 new perspectives for future studies, *Adv. in Meteorol.*, **2010**, 2010(3642), 1–
675 10, doi:10.1155/2010/310682,.

676

677 (7) Murphy, D. M., Froyd, K. D., Bian, H., Brock, C. A., Dibb, J. E., DiGangi,
678 J. P., Diskin, G., Dollner, M., Kupc, A., Scheuer, E. M., Schill, G. P., Weinzierl,
679 B., Iliamson, C. J., and Yu, P.: The distribution of sea-salt aerosol in the
680 global troposphere, *Atmos. Chem. Phys.*, 19, 4093-4104,
681 <https://doi.org/10.5194/acp-19-4093-2019>, 2019.

682

683 (8) Legrand, M., Preunkert, S., Wolff, E., Weller, R., Jourdain, B., and
684 Wagenbach, D.: Year-round records of bulk and size-segregated aerosol
685 composition in central Antarctica (Concordia site) – Part 1: Fractionation of
686 sea-salt particles, *Atmos. Chem. Phys.*, **2017**, 17, 14039-14054,
687 <https://doi.org/10.5194/acp-17-14039-2017>

688

689 (9) Huang, J., Jaeglé, L., and Shah, V.: Using CALIOP to constrain
690 blowing snow emissions of sea salt aerosols over Arctic and Antarctic sea ice,
691 *Atmos. Chem. Phys.*, **2018**, 18, 16253–16269, [https://doi.org/10.5194/acp-18-](https://doi.org/10.5194/acp-18-16253-2018)
692 16253-2018.

693

694 (10) Giordano, M. R., Kalnajs, L. E., Goetz, J. D., Avery, A. M., Katz, E.,
695 May, N. W., Leemon, A., Mattson, C., Pratt, K. A., and DeCarlo, P. F.: The

- 696 importance of blowing snow to halogen-containing aerosol in coastal
697 Antarctica: influence of source region versus wind speed, *Atmos. Chem.*
698 *Phys.*, **2018**, 18, 16689–16711, <https://doi.org/10.5194/acp-18-16689-2018>,
699
- 700 (11) Frey, M. M., Norris, S. J., Brooks, I. M., Anderson, P. S., Nishimura, K.,
701 Yang, X., Jones, A. E., Nerentorp Mastromonaco, M. G., Jones, D. H., and
702 Wolff, E. W.: First direct observation of sea salt aerosol production from
703 blowing snow above sea ice, *Atmos. Chem. Phys.*, **2020**, 20, 2549–2578,
704 <https://doi.org/10.5194/acp-20-2549-2020>.
705
- 706 (12) Charlson, R. J., Lovelock, J. E., Andreae, M. O. & Warren, S. G.
707 Oceanic phytoplankton, atmospheric sulphur, cloud albedo, and climate.
708 *Nature* **1987**, 326,655–661.
709
- 710 (13) Vallina, S. M., Simó, R., Gassó, S., de Boyer-Montégut, C., del Rio, E.,
711 Jurado, E., and Dachs, J, Analysis of a potential “solar radiation dose–
712 dimethylsulfide–cloud condensation nuclei” link from globally mapped
713 seasonal correlations, *Global Biogeochem. Cycles*, **2007**. 21, GB2004,
714 doi:10.1029/2006GB002787.
715
- 716 (14) Quinn, P. K. and Bates, T. S.: The case against climate regulation via
717 oceanic phytoplankton sulphur emissions, *Nature*, **2011**, 480(7375), 51–56,
718 doi:10.1038/nature10580
719
- 720 (15) Lana, A., Simó, R., Vallina, S. M. and Dachs, J.: Potential for a
721 biogenic influence on cloud microphysics over the ocean: a correlation study
722 with satellite-derived data, *Atmos. Chem. Phys.*, **2012**, 12(17), 7977–7993,
723 doi:10.5194/acp-12-7977-2012
724
- 725 (16) Quinn, P. K., Coffman, D. J., Johnson, J. E., Upchurch, L. M. & Bates,
726 T. S. Small fraction of marine cloud condensation nuclei made up of sea spray
727 aerosol. *Nature Geoscience*. **2017**, 10, 674–679
728 <https://doi.org/10.1038/ngeo3003>.
729
- 730 (17) Giordano, M. R., Kalnajs, L. E., Avery, A., Goetz, J. D., Davis, S. M.,
731 and DeCarlo, P. F.: A missing source of aerosols in Antarctica – beyond long-
732 range transport, phytoplankton, and photochemistry, *Atmos. Chem. Phys.*,
733 **2017**, 17, 1–20, <https://doi.org/10.5194/acp-17-1-2017>
734
- 735 (18) Sanchez, K. J., Chen, C.-L., Russell, L. M., Betha, R., Liu, J., Price, D.
736 J., Massoli, P., Ziemba, L. D., Crosbie, E. C., Moore, R. H., Mueller, M.,
737 Schiller, S. A., Wisthaler, A., Lee, A. K. Y., Quinn, P. K., Bates, T. S., Porter,
738 J., Bell, T. G., Saltzman, E. S., Vaillancourt, R. D. and Behrenfeld, M. J.:
739 Substantial seasonal contribution of observed biogenic sulfate particles to
740 cloud condensation nuclei, *Sci. Rep.*, **2018** 8(1):3235 doi:10.1038/s41598-
741 018-21590-9,.
742
- 743 (19) Rankin, A. M. and Wolff, E. W.: A year-long record of size segregated
744 aerosol composition at Halley, Antarctica, *J. Geophys. Res.*, **2003**, 108(D24),
745 4775, doi:4710.1029/2003JD003993.

746
747
748 (20) Legrand, M., Preunkert, S., Weller, R., Zipf, L., Elsässer, C., Merchel,
749 S., Rugel, G., and Wagenbach, D.: Year-round record of bulk and size-
750 segregated aerosol composition in central Antarctica (Concordia site) – Part 2:
751 Biogenic sulfur (sulfate and methanesulfonate) aerosol, *Atmos. Chem. Phys.*,
752 **2017**, 17, 14055-14073, <https://doi.org/10.5194/acp-17-14055-2017>,
753
754 (21) Simó, R. and Dachs, J.: Global ocean emission of dimethylsulfide
755 predicted from biogeophysical data, *Global Biogeochem. Cy.*, **2002** 16, 1018,
756 <https://doi.org/10.1029/2001GB001829>
757
758 (22) Gondwe, M., Krol, M., Klaassen, W., Gieskes, W., and de Baar, H.:
759 Comparison of modelled versus measured MSA: NSS SO₄ ratios: A global
760 analysis, *Global Biogeochem. Cy.*, 18, GB2006,
761 <https://doi.org/10.1029/2003GB002144>, 2004
762
763 (23) Meskhidze, N.; Nenes, A. Phytoplankton and cloudiness in the
764 Southern Ocean. *Science* **2006**, 314, 1419–1423.
765
766 (24) Korhonen, H., Carslaw, K. S., Spracklen, D. V., Mann, G., W., and
767 Woodhouse, M. T.: Influence of oceanic dimethyl sulfide emissions on cloud
768 condensation nuclei concentrations and seasonality over the remote Southern
769 Hemisphere oceans: A global model study, *J. Geophys. Res.-Atmos.*, **2008**,
770 113, D15204, doi:10.1029/2007JD009718,
771
772 (25) McCoy, D. T., Burrows, S. M., Wood, R., Grosvenor, D. P., Elliott, S. M.,
773 Ma, P.-L., Rasch, P. J., and Hartmann, D. L.: Natural aerosols explain
774 seasonal and spatial patterns of Southern Ocean cloud albedo, *Science*
775 *Advances* **2015**, 1, e1500157.
776
777 (26) Gras, J. L.; Keywood, M. Cloud condensation nuclei over the Southern
778 Ocean: wind dependence and seasonal cycles, *Atmos. Chem. Phys.* **2017**, 17,
779 4419–4432
780
781 (27) Fossum, K. N., Ovadnevaite, J., Ceburnis, D., Dall’Osto, M., Marullo, S.,
782 Bellacicco, M., Simó, R., Liu, D., Flynn, M., Zuend, A., O’Dowd, C.:
783 Summertime primary and secondary contributions to Southern Ocean cloud
784 condensation nuclei, *Scientific Reports.*, **2018**, 8, 13844
785
786 (28) O’Dowd, C. D., Facchini, M. C., Cavalli, F., Ceburnis, D., Mircea, M.,
787 Decesari, S., Fuzzi, S., Yoon, Y.-J. and Putaud, J.-P.: Biogenically driven
788 organic contribution to marine aerosol, *Nature* **2004**, 431(7009), 676–680,
789 doi:10.1038/nature02959,
790
791 (29) Virkkula, A., Teinilä, K., Hillamo, R., Kerminen, V.-M., Saarikoski, S.,
792 Aurela, M., Viidanoja, J., Paatero, J., Koponen, I. K., Kulmala, M.: Chemical
793 composition of boundary layer aerosol over the Atlantic Ocean and at an
794 Antarctic site, *Atmos. Chem. Phys.*, **2006**, 6, 3407–3421,
795

- 796 (30) Zorn, S. R., Drewnick, F., Schott, M., Hoffmann, T., Borrmann, S.:
797 Characterization of the South Atlantic marine boundary layer aerosol using an
798 aerodyne aerosol mass spectrometer, *Atmos. Chem. Phys.*, **2008** 8, 4711–
799 4728,
800
- 801 (31) Jung, J., Hong, S.-B., Chen, M., Hur, J., Jiao, L., Lee, Y., Park, K.,
802 Hahm, D., Choi, J.-O., Yang, E. J., Park, J., Kim, T.-W., and Lee, S.:
803 Characteristics of biogenically-derived aerosols over the Amundsen Sea,
804 Antarctica, *Atmos. Chem. Phys. Discuss.*, **2019**, [https://doi.org/10.5194/acp-](https://doi.org/10.5194/acp-2019-133)
805 2019-133. Manuscript under review for journal *Atmos. Chem. Phys.*
806 Discussion started: 20 March 2019
807
- 808 (32) Legrand, M., F. Ducroz, D. Wagenbach, R. Mulvaney, and J. Hall,
809 Ammonium in coastal Antarctic aerosol and snow: Role of polar ocean
810 and penguin emissions, *J. Geophys. Res.*, **1998**, 103, 11,043–11,056,
811 [doi:10.1029/97JD01976](https://doi.org/10.1029/97JD01976).
812
- 813 (33) Schmale, J., Schneider, J., Nemitz, E., Tang, Y. S., Dragosits, U.,
814 Blackall, T. D., Trathan, P. N., Phillips, G. J., Sutton, M., Braban, C. F.: Sub-
815 Antarctic marine aerosol: dominant contributions from biogenic sources,
816 *Atmos. Chem. Phys.*, **2013**, 13, 8669–8694.
817
- 818 (34) Liu, J., Dedrick, J., Russell, L. M., Senum, G. I., Uin, J., Kuang, C.,
819 Springston, S. R., Leaitch, W. R., Aiken, A. C., and Lubin, D.: High
820 summertime aerosol organic functional group concentrations from marine and
821 seabird sources at Ross Island, Antarctica, during AWARE, *Atmos. Chem.*
822 *Phys.*, **2018**, 18, 8571-8587, <https://doi.org/10.5194/acp-18-8571-2018>,
823
- 824 (35) Dall'Osto, M., Ovadnevaite, J., Paglione, M., Beddows, D.C.S.,
825 Ceburnis, D., Cree, C., Cortés, P., Zamanillo, M., Nunes, S.O., Pérez, G.L.,
826 Ortega-Retuerta, E., Emelianov, M., Vaqué, D., Marrasé, C., Estrada, M.,
827 Montserrat Sala, M., Vidal, M., Fitzsimons, M.F., Beale, R., Airs, R., Rinaldi,
828 M., Decesari, S., Facchini, M.C., Harrison, R.M., O'Dowd, C., Simó, R.,
829 Antarctic sea ice region as a source of biogenic organic nitrogen in aerosols.
830 *Sci. Rep.* **2017**, 7 6047. <https://doi.org/10.1038/s41598-017-06188-x>.
831
- 832 (36) Dall'Osto, M., Airs, R. L., Beale, R., Cree, C., Fitzsimons, M. F.,
833 Beddows, D., Harrison, R. M., Ceburnis, D., O'Dowd, C., Rinaldi, M., Paglione,
834 M., Nenes, A., Decesari, S., Simó, R.: Simultaneous detection of alkylamines
835 in the surface ocean and atmosphere of the Antarctic sympagic environment,
836 *ACS Earth Space Chem.*, **2019** 3, 5, 854-862.,
837
- 838 (37) Facchini, M. C., Decesari, S., Rinaldi, M., Carbone, C., Finessi, E.,
839 Mircea, M., Fuzzi, S., Moretti, F., Tagliavini, E., Ceburnis, D., O'Dowd, C. D.:
840 Important Source of Marine Secondary Organic Aerosol from Biogenic Amines,
841 *Environmental Science and Technology*, **2008**, 42, 9116 – 9121.
842
- 843 (38) McMurry, P. H. A review of atmospheric aerosol measurements. *Atmos.*
844 *Environ.* **2000**, 34, 1959-1999
845

- 846 (39) Huang, S., Wu, Z., Poulain, L., van Pinxteren, M., Merkel, M., Assmann,
847 D., Herrmann, H., and Wiedensohler, A.: Source apportionment of the organic
848 aerosol over the Atlantic Ocean from 53°N to 53°S: significant contributions
849 from marine emissions and long-range transport, *Atmos. Chem. Phys.*, **2018**,
850 18, 18043–18062, <https://doi.org/10.5194/acp-18-18043-2018>,
851
- 852 (40) Song, X. H., Hopke, P. K., Fergenson, D. P., and Prather, K. A.:
853 Classification of single particles analyzed by ATOFMS using an artificial
854 neural network, ART-2A, *Anal. Chem.*, **1999** 71, 860–865,
855
- 856 (41) DeCarlo, P. F., Kimmel, J. R., Trimborn, A., Northway, M. J., Jayne, J.
857 T., Aiken, A. C., Gonin, M., Fuhrer, K., Horvath, T., Docherty, K. S., Worsnop,
858 D. R., and Jimenez, J. L.: Field-Deployable, High-Resolution, Time-of-Flight
859 Aerosol Mass Spectrometer, *Anal. Chem.*, **2006**, 78, 8281–8289.
860
- 861
- 862 (42) Decesari, S., Paglione, M., Rinaldi, M., Dall'Osto, M., Simó, R., Zanca,
863 N., Volpi, F., Facchini, M. C., Hoffmann, T., Götz, S., Kampf, C. J., O'Dowd,
864 C., Ceburnis, D., Ovadnevaite, J., and Tagliavini, E.: Shipborne
865 measurements of Antarctic submicron organic aerosols: an NMR perspective
866 linking multiple sources and bioregions, *Atmos. Chem. Phys.*, **2020**, 20, 4193–
867 4207, <https://doi.org/10.5194/acp-20-4193-2020>
868
- 869 (43) Lana, A., Bell, T. G., Simó, R., Vallina, S. M., Ballabrera-Poy, J., Kettle,
870 A. J., Dachs, J., Bopp, L., Saltzman, E. S., Stefels, J., Johnson, J. E., and Liss,
871 P. S.: An updated climatology of surface dimethylsulfide concentrations and
872 emission fluxes in the global ocean, *Global Biogeochem. Cycles*, **2011**, 25,
873 GB1004, doi:10.1029/2010gb003850.
874
- 875 (44) Rinaldi, M., Decesari, S., Carbone, C., Finessi, E., Fuzzi, S., Ceburnis,
876 D., O'Dowd, C. D., Sciare, J., Burrows, J. P., Vrekoussis, M., Ervens, B.,
877 Tsigaridis, K., Facchini, M. C.: Evidence of a natural marine source of oxalic
878 acid and a possible link to glyoxal. *J. Geophys. Res. Atmos.* **2011** 116.
879 D16204, <http://dx.doi.org/10.1029/2011JD015659>
880
- 881 (45) Sorooshian, A., Brechtel, F. J., Ervens, B., Feingold, G., Varutbangkul,
882 V., Bahreini, R., Murphy, S., Holloway, J. S., Atlas, E. L., Anlauf, K., Buzorius,
883 G., Jonsson, H., Flagan, R. C., and Seinfeld, J. H.: Oxalic acid in clear and
884 cloudy atmospheres: Analysis of data from International Consortium for
885 Atmospheric Research on Transport and Transformation 2004, *J. Geophys.*
886 *Res.*, **2006**, 111, D23, doi:10.1029/2005JD006880,
887
- 888 (46) Miyazaki, Y., Kawamura, K., and Sawano, M.: Size distributions and
889 chemical characterization of water soluble organic aerosols over the western
890 North Pacific in summer, *J. Geophys. Res.*, **2010**, 115, D23210,
891 doi:10.1029/2010JD014439.
892
- 893 (47) Mochida, M., Umemoto, N., Kawamura, K., and Uematsu, M.: Bimodal
894 size distribution of C₂–C₄ dicarboxylic acids in the marine aerosols, *Geophys.*
895 *Res. Lett.*, **2003**, 30(13), 1672, doi:10.1029/2003GL017451.

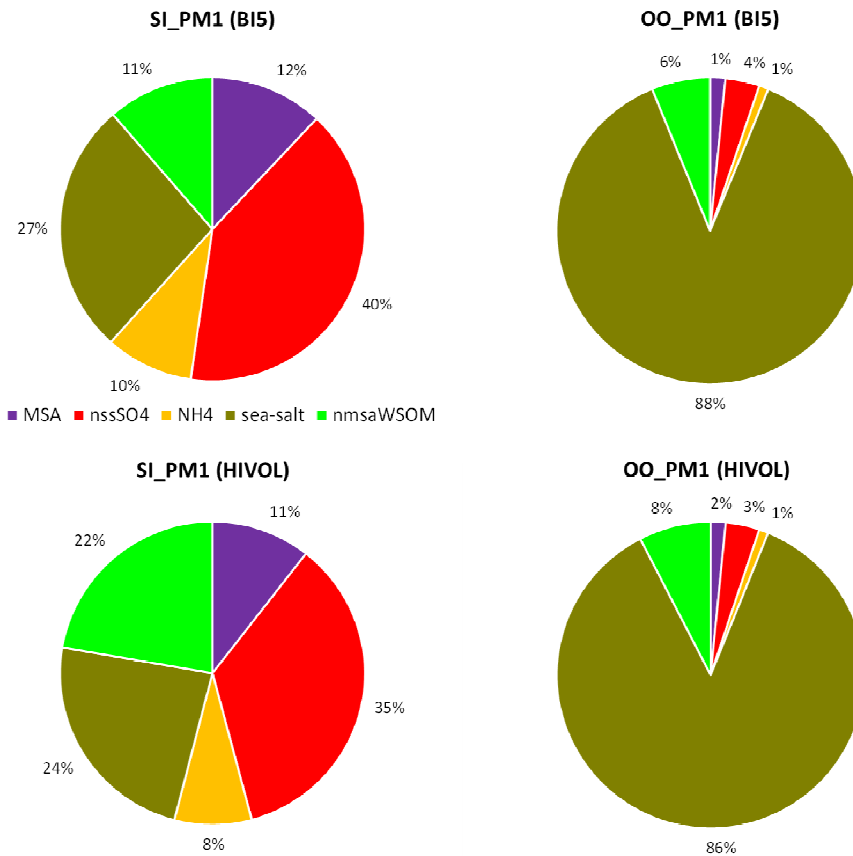
896
897 (48) Kawamura, K., and F. Sakaguchi, Molecular distributions of water
898 soluble dicarboxylic acids in marine aerosols over the Pacific Ocean including
899 tropics, *J. Geophys. Res.*, **1999**, 104(D3), 3501–3509,
900 doi:10.1029/1998JD100041
901
902
903 (49) Xu, G., Y. Gao, Q. Lin, W. Li, and L. Chen, Characteristics of water-
904 soluble inorganic and organic ions in aerosols over the Southern Ocean and
905 coastal East Antarctica during austral summer, *J. Geophys. Res. Atmos.*,
906 **2013** 118,13,303–13,318, doi:10.1002/2013JD019496
907
908 (50) Wang, H., K. Kawamura, and K. Yamazaki, Water-soluble dicarboxylic
909 acids, ketoacids and dicarbonyls in the atmospheric aerosols over the
910 Southern Ocean and western Pacific Ocean, *J. Atmos. Chem.*, **2006**, 53(1),
911 43–61,doi:10.1007/s10874-006-1479-4.
912
913 (51) Sullivan R. C. and Prather, K. A.: Investigations of the diurnal cycle and
914 mixing state of oxalic acid in individual particles in Asian aerosol outflow,
915 *Environ. Sci. Technol.*, **2007**, 41, 8062–8069.
916
917 (52) Fergenson, D.P., Pitesky, M.E., Tobias, H.J., Steele, P.T., Czerwieniec,
918 G.A., Russell, D.H., Lebrilla, C.B., Horn, J.M., Coffee, K.R., Srivastava, A.,
919 Pillai, S.P., Shih, M.-T., Hall, H.L., Ramponi, A.J., Chang, J.T., Langlois, R.G.,
920 Estacio, P.L., Hadley, R.T., Frank, M., Gard, E.E. Reagentless detection and
921 classification of individual bioaerosol particles in seconds. *Anal. Chem.*, **2004**,
922 76, 373–378.
923
924 (53) Pratt, K., DeMott, P.J., French, J.R., Wang, Z., Westphal, D.L.,
925 Heymsfield, A.J., Twohy, C.H., Prenni, A.J., Prather, K.A.,. Situ detection of
926 biological particles in cloud ice-crystals. *Nat. Geosci.* **2009**, 2, pages398–401
927 <https://doi.org/10.1038/ngeo521>
928
929 (54) Healy, R.M., Evans, G.J., Murphy, M., Sierau, B., Arndt, J.,
930 McGillicuddy, E., O'Connor, I.P., Sodeau, J.R., Wenger, J.C., Single-particle
931 speciation of alkylamines in ambient aerosol at five European sites. *Anal.*
932 *Bioanal. Chem.* **2015**, 407, 5899–5909
933
934 (55) Dall'Osto, M., Beddows, D. C. S., McGillicuddy, E. J., Esser-Gietl, J. K.,
935 Harrison, R. M., and Wenger, J. C., On the simultaneous deployment of two
936 single-particle mass spectrometers at an urban background and a roadside
937 site during SAPUSS, *Atmos. Chem. Phys.*, **2016**, 16, 9693-9710,
938 <https://doi.org/10.5194/acp-16-9693-2016>.
939
940 (56) Rehbein PJG, Jeong C-H, McGuireML, Yao X, Corbin JC, EvansGJ
941 Cloud and fog processing enhanced gas-to-particle partitioning of
942 trimethylamine. *Environ Sci Technol* **2011**, 45(10):4346– 4352.
943 doi:10.1021/es1042113
944

- 945 (57) Murphy S.M., Sorooshian A., Kroll J.H., Ng N.L., Chhabra P., Tong C.,
946 Surratt J.D., Knipping E., Flagan R.C., Seinfeld J.H., Secondary aerosol
947 formation from atmospheric reactions of aliphatic amines. *Atmos. Chem. Phys.*
948 2007, 7(9):2313–2337
949
- 950 (58) Whiteaker, J. R. and Prather, K. A.: Hydroxymethanesulfonate as a
951 tracer for fog processing of individual aerosol particles, *Atmos. Environ.*, **2003**,
952 37, 1033–1043
953
- 954 (59) Dall'Osto, M., Harrison, R. M., Coe, H., and Williams, P.: Real-time
955 secondary aerosol formation during a fog event in London, *Atmos. Chem.*
956 *Phys.*, **2009**, 9, 2459–2469, <https://doi.org/10.5194/acp-9-2459-2009>,
957
- 958 (60) Angelino, S.; Suess, D. T.; Prather, K. A. Formation of aerosol particles
959 from reactions of secondary and tertiary alkylamines: Characterization by
960 aerosol time-of-flight mass spectrometry. *Environ. Sci. Technol.* **2001**, 35,
961 3130–3138.
962
- 963 (61) Jokinen, T., Sipilä, M., Kontkanen, J., Vakkari, V., Tisler, P., Duplissy,
964 E.-M., Junninen, H., Kangasluoma, J., Manninen, H. E., Petäjä, T., Kulmala,
965 M., Worsnop, D. R., Kirkby, J., Virkkula, A., and Kerminen, V.-M.: Ion-induced
966 sulfuric acid–ammonia nucleation drives particle formation in coastal
967 Antarctica, *Sci. Adv.*, **2018**, 4, eaat9744,
968 <https://doi.org/10.1126/sciadv.aat9744>,
969
- 970 (62) Kawamura, K., R. Seméré, Y. Imai, Y. Fujii, and M. Hayashi, Water
971 soluble dicarboxylic acids and related compounds in Antarctic aerosols,
972 *J. Geophys. Res.*, **1996**, 101(D13), 18,721–18,728, doi:10.1029/96JD01541.
973
- 974 (63) Kawamura, K., H. Kasukabe, and L. A. Barri, Source and reaction
975 pathways of dicarboxylic acids, ketoacids and dicarbonyls in Arctic aerosols:
976 One year of observations, *Atmos. Environ.*, **1996**, 30(10–11), 1709–1722,
977 doi:10.1016/1352-2310(95)00395-9.
978
- 979 (64) Kerminen, V. - M., K. Teinilä, R. Hillamo, and T. Mäkel, Size segregated
980 chemistry of particulate dicarboxylic acids in the Arctic atmosphere, *Atmos.*
981 *Environ.*, **1999**, 33, 2089–2100, doi:10.1016/S1352- 2310(98)00350-1.
982
983
- 984 (65) Matsumoto, K., I. Nagao, H. Tanaka, H. Miyaji, T. Iida, and Y. Ikebe,
985 Seasonal characteristics of organic and inorganic species and their size
986 distributions in atmospheric aerosols over the northwest Pacific Ocean, *Atmos.*
987 *Environ.*, **1998**, 32 (11), 1931–1946, doi:10.1016/S1352-2310(97)00499-8.
988
- 989 (66) Warneck, P. In - cloud chemistry opens pathway to the formation of
990 oxalic acid in the marine atmosphere, *Atmos. Environ.*, **2003**, 37, 2423–2427,
991 doi:10.1016/S1352-2310(03)00136-5.
992

- 993 (67) Crahan, K. K., D. Hegg, D. S. Covert, and H. Jonsson, An exploration
994 of aqueous oxalic acid production in the coastal marine atmosphere, *Atmos.*
995 *Environ.*, **2004**, 38, 3757–3764, doi:10.1016/j.atmosenv.2004.04.009.
996
- 997 (68) Turekian, V. C., S. A. Macko, and W. C. Keene, Concentrations,
998 isotopic compositions, and sources of size - resolved, particulate organic
999 carbon and oxalate in near - surface marine air at Bermuda during spring, *J.*
1000 *Geophys. Res.*, **2003**, 108(D5), 4157, doi:10.1029/2002JD002053.
1001
- 1002
- 1003 (69) Pye, H. O. T., Nenes, A., Alexander, B., Ault, A. P., Barth, M. C., Clegg,
1004 S. L., Collett Jr., J. L., Fahey, K. M., Hennigan, C. J., Herrmann, H.,
1005 Kanakidou, M., Kelly, J. T., Ku, I.-T., McNeill, V. F., Riemer, N., Schaefer, T.,
1006 Shi, G., Tilgner, A., Walker, J. T., Wang, T., Weber, R., Xing, J., Zaveri, R. A.,
1007 and Zuend, A.: The acidity of atmospheric particles and clouds, *Atmos. Chem.*
1008 *Phys.*, **2020**, 20, 4809–4888, <https://doi.org/10.5194/acp-20-4809-2020>.
1009
- 1010 (70) Hoppel, W.A., Frick, G.M., Fitzgerald, J.W.,. Marine boundary layer
1011 measurements of new-particle formation and the effects of non-precipitating
1012 clouds have on aerosol size distribution. *J. Geophys. Res.* **1994**, 99, 14443–
1013 14459
1014
- 1015 (71) Kim, H., Collier, S., Ge, X., Xu, J., Sun, Y., Jiang, W., Wang, Y.,
1016 Herckes, P., and Zhang, Q.: Chemical processing of water soluble species
1017 and formation of secondary organic aerosol in fogs, *Atmos. Environ.*, **2019**,
1018 200, 158–166.
1019
- 1020 (72) Legrand, M., V. Gros, S. Preunkert, R. Sarda-Estève, A.-M. Thierry, G.
1021 Pépy, and B. Jourdain, A reassessment of the budget of formic and acetic
1022 acids in the boundary layer at Dumont d’Urville (coastal Antarctica): The role
1023 of penguin emissions on the budget of several oxygenated volatile organic
1024 compounds, *J. Geophys. Res.*, **2012**, 117, D06308,
1025 doi:10.1029/2011JD017102
1026
- 1027 (73) Speir, T. W., and J. C. Cowling. Ornithogenic soils of the Cape Bird
1028 Adelie penguin rookeries, Antarctica. 1. Chemical properties, *Polar Biol.*, **1984**
1029 2, 199–205, doi:10.1007/BF00263625.
1030
- 1031 (74) Speir, T. W., and R. J. Ross , Ornithogenic soils of the Cape Bird
1032 Adelie penguin rookeries, Antarctica. 2. Ammonia evolution and enzyme
1033 activities, *Polar Biol.*, **1984**, 2, 207–212, doi:10.1007/BF00263626.
1034
- 1035 (75) Jourdain, B., and M. Legrand. Year-round records of bulk and size
1036 segregated aerosol composition and HCl and HNO₃ levels in the Dumont
1037 d’Urville (coastal Antarctica) atmosphere: Implications for sea-salt aerosol in
1038 the winter and summer, *J. Geophys. Res.*, **2002**, 107(D22), 4645,
1039 doi:10.1029/2002JD002471
1040
- 1041 (76) Convey P, Chown SL, Clarke A, Barnes DKA, Cummings V, Ducklow H,
1042 Frati F, Green TGA, Gordon S, Griffiths H, Howard-Williams C, Huiskes AHL,

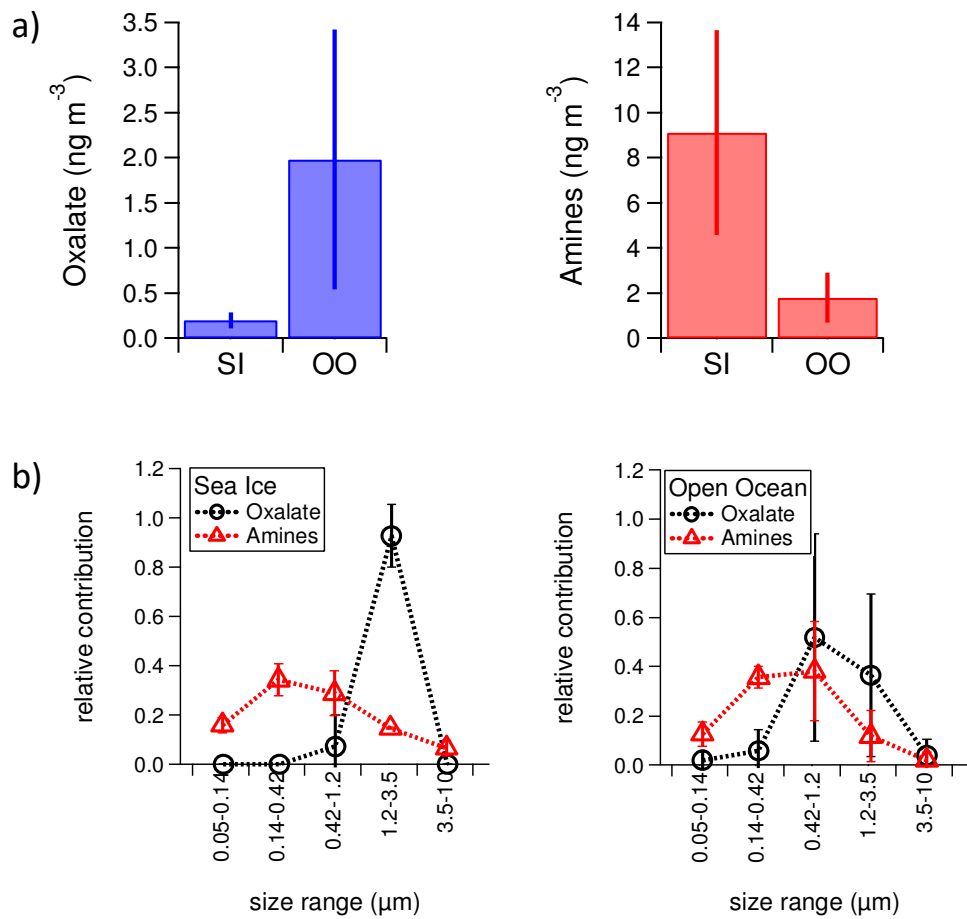
1043 Laybourn-Parry J, Lyons B, McMinn A, Peck LS, Quesada A, Schiaparelli S,
1044 Wall D. The spatial structure of Antarctic biodiversity. *Ecol Monogr* **2014**,
1045 84:203–244
1046
1047
1048 (77) Rintoul, S. R., Chown, S. L., DeConto, R. M., England, M. H., Fricker, H.
1049 A., Masson-Delmotte, V., Naish, T. R., Siegert, M. J., and Xavier, J. C.:
1050 Choosing the future of Antarctica. *Nature* **2018** 558, 233–241. doi:
1051 10.1038/s41586-018-0173-4
1052
1053 (78) Lee, J.R., Raymond, B., Bracegirdle, T.J., Chadès, I., Fuller, R.A.,
1054 Shaw, J.D., Terauds, A., Climate change drives expansion of Antarctic ice-
1055 free habitat. *Nature* **2017**, 547, 49–54.
1056
1057 (79) Sulzberger, B., Austin, A. T., Cory, R. M., Zepp, R. G., and Paul, N. D.:
1058 Solar UV radiation in a changing world: roles of cryosphere-land-water-
1059 atmosphere interfaces in global biogeochemical cycles, *Photochem. Photobio.*
1060 **2019** S., 18, 747–774, <https://doi.org/10.1039/c8pp90063a>,.
1061
1062
1063
1064
1065
1066
1067
1068
1069
1070
1071
1072
1073
1074
1075
1076
1077
1078
1079
1080
1081
1082
1083
1084
1085
1086
1087
1088
1089
1090
1091
1092

1093
1094
1095
1096
1097
1098
1099



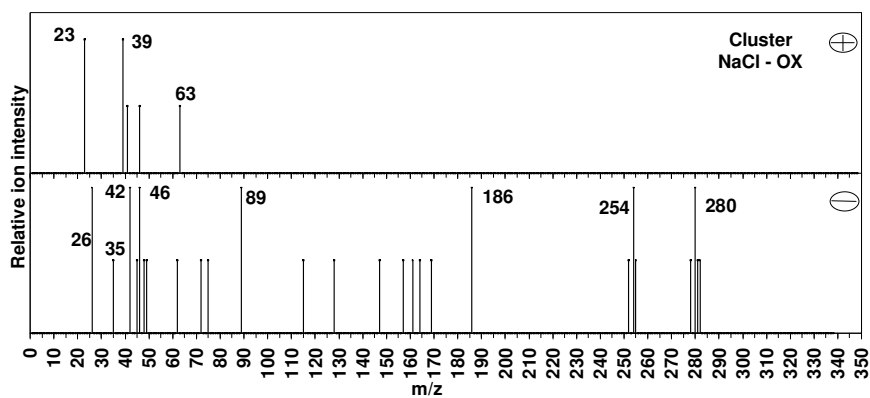
1100
1101
1102
1103
1104
1105
1106
1107
1108
1109
1110
1111

Figure 1. Composition of PM₁ aerosol water soluble fraction in the sea ice influenced region (SI) versus open ocean (OO). The “BI5” pies refer to measurements performed on Berner impactor, while the “HIVOL” pies refers to the WSOM measured on the high volume samples; nmsaWSOM stands for non-MSA-WSOM.



1112
 1113 **Figure 2.** (a) PM₁₀ concentrations of oxalate and amines in SI and OO
 1114 samples (average and standard deviation). (b) Normalized size distributions of
 1115 oxalate and amines for the 2 regions.

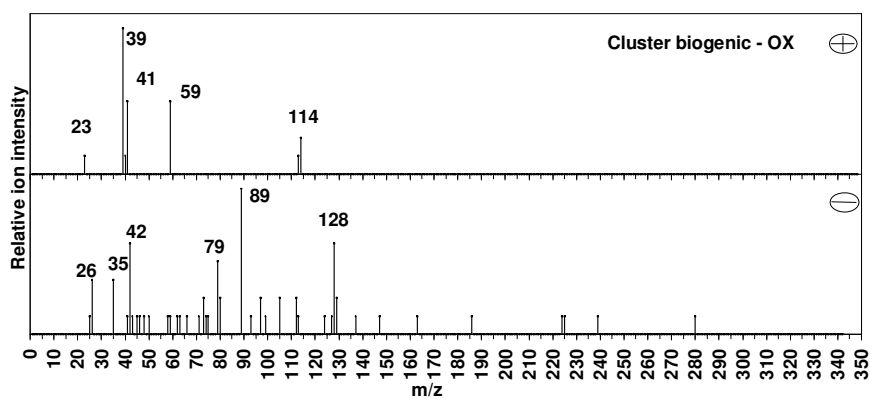
1116



1117

1118

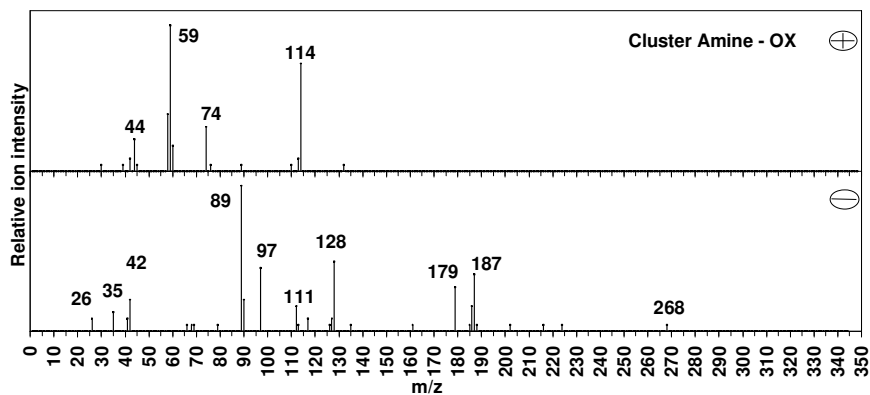
(a)



1119

1120

(b)



1121

1122

1123

1124 **Figure 3** Average Art-2a positive and negative mass spectra for (a)ATOFMS

1125 oxalate internally mixed with sea spray, (b) ATOFMS oxalate in biogenic

1126 particles and (c) ATOFMS oxalate in secondary organic aerosols

1127

(c)